Journal of Power Sources 196 (2011) 4705–4713

Contents lists available at ScienceDirect

Journal of Power Sources

journal homepage: www.elsevier.com/locate/jpowsour

Evaluation of Tafel–Volmer kinetic parameters for the hydrogen oxidation reaction on Pt(1 1 0) electrodes

R.F. Mann, C.P. Thurgood*

Department of Chemistry and Chemical Engineering, Royal Military College of Canada, P.O. Box 17000, Station Forces, Kingston, Ontario, K7K 7B4 Canada

ARTICLE INFO

Article history:
Received 25 June 2010
Received in revised form
10 December 2010
Accepted 13 December 2010
Available online 21 December 2010

Keywords:
Hydrogen oxidation reaction
Pt(1 1 0) electrodes
Anode polarization
Activation polarization
PEM fuel cells
Modelling

ABSTRACT

Modelling of PEM fuel cells has long been an active research area to improve understanding of cell and stack operation, facilitate design improvements and support simulation studies. The prediction of activation polarization in most PEM models has concentrated on the cathode losses since anode losses are commonly much smaller and tend to be ignored. Further development of the anode activation polarization term is being undertaken to broaden the application and usefulness of PEM models in general.

Published work on the kinetics of the hydrogen oxidation reaction (HOR) using Pt($h\,k\,l$) electrodes in dilute H_2SO_4 has been recently reassessed and published. Correlations for diffusion-free exchange current densities were developed and empirical predictive equations for the anode activation polarization were proposed for the experimental conditions of the previously published work: Pt(1 0 0), Pt(1 1 0) and Pt(1 1 1) electrodes, p_{H_2} of 1 atm, and temperatures of 1, 30 and 60 °C. It was concluded that the HOR on Pt(1 1 0) electrodes followed a Tafel–Volmer reaction sequence.

The aim of the present paper is to generalize these Tafel–Volmer correlations, apply them to published data for Pt(1 1 0) electrodes and further develop the modelling of anode activation polarization over the range of operating conditions found in PEMFC operation.

1. Introduction

The background for the present paper has been recently published [1–3]. Our long-term aim is to further develop our generalized steady-state electrochemical model, the GSSEM, which consists of a simple, 1-dimensional, model of a PEM fuel cell (PEMFC) based on

$$V = E + \eta_{act,a} + \eta_{act,c} + \eta_{ohmic} + \eta_{conc,a} + \eta_{conc,c} \quad (1)$$

The specific goal of the present paper is to further evaluate previously published work which studied the hydrogen oxidation reaction on Pt($h\,k\,l$) electrodes in dilute H_2SO_4 and to develop the results into a modelling approach for $\eta_{act,a}$, the anode activation polarization, in PEMFCs. The quantitative prediction of this particular loss is generally not given much attention in a PEMFC model since it is, normally, much less significant than the corresponding loss at the cathode. There are situations, however, where the anode activation polarizations could become significant and a modelling capability is therefore desirable.

Our present interest is the anode activation polarization related to the 'hydrogen oxidation reaction' (HOR) for which the overall half-cell reaction is

$$H_2 \Rightarrow 2H^+ + 2e^- \quad (2)$$

The reverse of reaction (2) is the 'hydrogen evolution reaction' (HER).

The anode reaction occurs in the presence of a catalyst, typically Pt if the anode feedstock is pure hydrogen.

There is broad support in the literature for the HOR on Pt to proceed via a Tafel–Volmer reaction sequence, fully described recently [3]. There is not, however, complete agreement on the kinetic model as literature support exists for both 'rds Tafel–fast Volmer' kinetics and for 'fast Tafel–rds Volmer' kinetics. These were respectively referred to as 'Mechanism I' and 'Mechanism II' in our recent reassessment [3] of a body of work published by what we chose to call the 'Markovic Group' [4–9]. This group of publications included extensive results for rotating disk electrode (RDE) studies of the HOR on single-crystal Pt(1 0 0), Pt(1 1 0) and Pt(1 1 1) electrodes in dilute sulphuric acid electrolyte at 1, 30 and 60 °C and 'corrected to a p_{H_2} of 1 atm'. These publications [4–9] concluded that the Pt(1 1 0) results were best explained by 'rds Tafel–fast Volmer' kinetics, our so-called 'Mechanism I'.

The present paper, in Section 2, will review the detailed development of thermodynamic and kinetic equations for 'Mechanism

* Corresponding author at: Department of Chemistry and Chemical Engineering, Royal Military College of Canada, 11 General Crerar Crescent, Kingston, Ontario, K7K 7B4 Canada. Tel.: +1 613 541 6000x6981; fax: +1 613 542 9489.
E-mail address: thurgood-c@rmc.ca (C.P. Thurgood).

0378-7753/$ – see front matter.
doi:10.1016/j.jpowsour.2010.12.016

Nomenclature

b	Tafel slope, $2.3RT(\alpha F)^{-1}$ (V dec^{-1})
B–V	Butler–Volmer
c	concentration (mol cm^{-3})
c_{H_2}	concentration of dissolved hydrogen at the reaction interface (mol H_2 cm^{-3})
C_M	concentration of active Pt sites [in sites cm^{-2} (order 10^{15}) or moles of sites cm^{-2} (order 10^{-8})]
E	equilibrium EMF of a cell (V) or total anode polarization, $\eta_{act,a} + \eta_{conc,a}$, in Refs. [4–9] (V)
$f_I(\theta,\theta_0)$	functions of θ and θ_0 in the general Butler–Volmer equation (see following Eq. (25))
F	Faraday's Constant (clbs equ't^{-1})
GSSEM	generalized steady state electrochemical model
H	Henry's Law 'constant' (atm cm^3 mol^{-1})
HER	hydrogen evolution reaction (reverse of Eq. (2))
HOR	hydrogen oxidation reaction (Eq. (2))
i	current density (A cm^{-2})
i_o	exchange current density (A cm^{-2})
k	chemical rate constant
k_{ads}	rate constant for the 2-site dissociative chemisorption of a hydrogen molecule [cm^5 s^{-1} (mol of vacant Pt sites)$^{-2}$]
k_{des}	rate constant for the hydrogen molecule desorption reaction [(mol H_2) cm^2 s^{-1} (mol of occupied Pt sites)$^{-2}$]
$k_{et,fwd}$	forward rate constant for the electron transfer (Vogel) reaction
$k_{et,rev}$	reverse rate constant for the electron transfer (Vogel) reaction
K_{ads}	adsorption equilibrium constant for chemisorbed hydrogen molecules (also equal to k_{ads}/k_{des}) [cm^3 (mol H_2)$^{-1}$, the reciprocal of the units of c_{H_2}]
$K_{et}c_{H_3O^+,o}$	equilibrium 'constant', representing $\{k_{-et}c_{H_3O^+,o}(k_{et})^{-1}\}$, for the electron transfer reactions, Eqs. (8) and (9)
Mechanism I	the 'rds Tafel–fast Volmer' HOR process
n	number of electrons being transferred for one act of the overall reaction
n_a	number of electrons being transferred 'after' the rds
n_b	number of electrons being transferred 'before' the rds
p	partial pressure of a gas component (atm)
r	chemical reaction rate
rds	rate-determining-step in the reaction sequence at the anode
RDE	rotating disk electrode
V	cell voltage (V)

Greek letters

α	transfer coefficient
β	symmetry factor
η	polarization (i.e. overvoltage or loss) (V)
θ	fractional surface coverage (generally of chemisorbed hydrogen atoms)
ν	stoichiometric coefficient in Eq. (5) (number of times that the rds must take place for the overall reaction to occur once)

Subscripts

a	anode or activity
act	activation
ads	adsorption
b	bulk
c	cathode
conc	concentration (relating to mass transfer losses)
des	desorption
et	electron transfer (as in the Volmer reaction)
expl	experimental
fwd	forward
H_2	hydrogen molecule
H	hydrogen atom
H_3O^+	hydrated proton (i.e. H^+:H_2O)
i	interface
I	Mechanism I
MG	Markovic Group (authors of Refs. [4–8])
ohmic	relating to ohmic (i.e. iR) losses
o	at zero polarization and zero net current condition (i.e. at equilibrium)
pred	predicted
rev	reverse
sat	saturated
T	Tafel reaction
V	Volmer reaction
vac	vacant

I', the 'rds Tafel–fast Volmer' HOR process. Then, in Section 3, these equations will be applied to the further analysis and correlation/recorrelation of some published results for the HOR on Pt(1 1 0) electrodes and evaluation of the Tafel–Volmer, T–V, parameters. Section 4 will then deal briefly with the generalization of these correlations to values of p_{H_2} and temperatures that are more representative of PEMFC modelling applications.

2. Development of mechanistic equations for a 'Tafel–Volmer' HOR reaction

2.1. Introduction

The basic theories of activation polarizations for the HOR and, especially, overvoltages for the HER have been established for decades. This section will summarize the development of a correlation and modelling approach for the anode activation polarization that is as mechanistic as possible yet as simple to understand and apply as possible. The goal is to develop a relationship linking the anode activation polarization to the current density and the other operating parameters of the fuel cell.

The literature dealing with both the HOR and the HER is vast but there appears to be general agreement on the main features of the process. Much of the following development has benefited from the previous work of Parsons [10], Austin [11,12], Bockris and Reddy [13], Gileadi et al. [14], the 'Markovic Group' [4–9], Springer et al. [15], Camara et al. [16], Breiter [17] and Lasia [18].

2.2. Fundamental steps in the HOR

Various possible steps in the overall HOR have been suggested, one combination being the so-called 'Tafel–Volmer sequence'. Using 'M' to represent an active Pt atom and 'e$^-$' to represent an electron, the steps in this sequence are:

(i) $H_2 + M \Leftrightarrow M.H_2$
(ii) $M.H_2 + M \Leftrightarrow 2M.H$
with (i) + (ii), the 'Tafel step', often simply
(iii) $H_2 + 2M \Leftrightarrow H_{ad} + H_{ad}$

(iv) $M.H + H_2O \Leftrightarrow H_3O^+ + M + e^-$
(v) $H_3O^+ \Leftrightarrow H^+ + H_2O$
with (iv) + (v), the 'Volmer step', often simply
(vi) $H_{ad} \Leftrightarrow H^+ + e^-$

2.3. The physical picture

At the gas/electrolyte interface, a hydrogen gas partial pressure, p_{H_2}, is in equilibrium with concentration $c_{H_2,sat}$ of dissolved hydrogen according to a Henry's Law equilibrium expression. Dissolved hydrogen will undergo bulk diffusion through the electrolyte to the vicinity of the anode, delivering a bulk concentration $c_{H_2,b}$ at the electrolyte/reaction boundary layer interface. If the mass transfer through the electrolyte is very rapid, or if it has been accounted for by subtracting the anode concentration polarization from the total anode polarization, $c_{H_2,b}$ can be taken as equal to $c_{H_2,sat}$. The dissolved hydrogen concentration at the reaction interface, $c_{H_2,i}$ (or, simply, c_{H_2}) may be different than $c_{H_2,b}$. Likewise, the proton concentration at the reaction interface will be denoted as $c_{H_3O^+}$ and that at the interface between the electrical boundary layer and the bulk electrolyte will be $c_{H_3O^+,b}$. Again, $c_{H_3O^+}$ may have a value different than $c_{H_3O^+,b}$. Just as $c_{H_2,b}$ is a function of factors external to the reaction boundary layer, so will $c_{H_3O^+,b}$ depend on factors external to the electrical boundary layer, e.g. the diffusion rate of the hydrated protons through the electrolyte. At the zero-current/zero-polarization situation, c_{H_2} and $c_{H_3O^+}$ at the reaction interface will be denoted as $c_{H_2,o}$ and $c_{H_3O^+,b}$, respectively.

2.4. Kinetic expressions for the Tafel and Volmer reactions

Kinetic expressions, initially in terms of the chemical reaction rate '*r*', for the above reactions can initially be written in their simplest form as follows, essentially using the nomenclature in Breiter [17] and applying Langmuir–Hinshelwood methodology:

For the Tafel, 'adsorption/desorption', reaction involving 1 molecule of H_2:

$$r_T = r_{T,ads} - r_{T,des} = k_{T,fwd} a_{H_2} (1-\theta_H)^2 - k_{T,rev}\theta_H^2 \quad (3)$$

For the Volmer, 'electron transfer or ionization', reaction, which would have to occur twice (i.e. a stoichiometric number of 2) per molecule of H_2:

$$r_V = r_{V,fwd} - r_{V,rev} = k_{V,fwd}\theta_H \exp[\alpha_{V,fwd}\eta F(RT)^{-1}] - k_{V,rev}(1-\theta_H)a_{H^+}\exp[-\alpha_{V,rev}\eta F(RT)^{-1}] \quad (4)$$

In Eqs. (3) and (4), the rate constants, k_i, will include some parameter to represent the catalyst concentration.

The transfer coefficient, α, has recently been discussed [2,3] and can generally be expressed as a function of β, the symmetry factor. Based on earlier work, the following expression was proposed by Gileadi et al. [14] with the symbols and subscripts as defined in the Nomenclature:

$$\alpha = [\beta(n - n_b - n_a) + n_b](\nu)^{-1} \quad (5)$$

In kinetic expressions involving catalyst concentration, the fraction of the Pt sites that are vacant is often required. This leads to the introduction of the common Langmuir–Hinshelwood parameter, θ_{vac}, the fraction of the active sites that is vacant and therefore able to participate in the chemisorption/dissociation reactions on each electrode. For a feed that is free of impurities, this should simply depend on the fraction of the sites occupied by adsorbed H atoms, $\theta_{H_{ads}}$, i.e. $\theta_{vac} = 1 - \theta_{H_{ads}}$. Since the present paper considers that 'H' (i.e. H_{ads}) is the only adsorbed species, θ will be understood to mean $\theta_{H_{ads}}$.

Mechanistic equations for the general Tafel–Volmer reaction sequence will now be developed in detail, enlarging on and modifying the Eqs. (3) and (4) proposed by Breiter and utilizing the detailed treatment in Section 5.9.3 of Austen [11]. The special case, Mechanism I, 'rds Tafel followed by fast Volmer', will then be developed from these general equations.

2.5. Tafel–Volmer equations for the HOR

2.5.1. Introduction

The following development of equations to describe the HOR is based on chemisorption according to a Langmuir isotherm, i.e. active Pt sites energetically homogeneous and no interactions between adsorbed species. Although 'ideal' Langmuir adsorption is often assumed because of the relative simplicity of the resulting kinetic equations, the Markovic Group, in fact, did study the chemisorption of hydrogen on the various Pt(*h k l*) crystal faces. Their study [5], in conjunction with the earlier work of Vetter [19], concluded that, although the Pt(1 1 1)data were best fitted by a non-ideal Frumkin isotherm, "the HOR on Pt(1 1 0) at low overpotentials followed application of the Langmuir ideal adsorption isotherm of H_{ads} and the ideal dual-site form of the Tafel–Volmer sequence, the atom-atom recombination step (i.e. the reverse Tafel reaction) being the rds." In addition, they concluded for Pt(1 1 0) "that the kinetics and mechanisms of the HER and HOR should be the same".

The '*nF*' conversion from a chemical rate equation (mole-based) to an electrochemical rate equation (current-based) is now added. Parameter C_M represents the active catalyst concentration at the reaction interface. Typically, for low-pressure and near ideal behaviour, activities can be replaced by the corresponding concentrations. The a_{H_2} in Eq. (3) will, therefore, be replaced by the hydrogen partial pressure, p_{H_2}, or, more appropriately for a liquid-phase reaction, c_{H_2}, the concentration of dissolved hydrogen in the electrolyte at the reaction interface. Similarly, the a_{H^+} in Eq. (4) will be replaced by $c_{H_3O^+}$, the concentration of the hydrated protons at the reaction interface.

2.5.2. The Tafel reaction for dissociative chemisorption

Eq. (3), with '$n = 2$' and with the refinements described above, leads to the rates of adsorption and desorption (per unit catalyst surface area), expressed as current densities, as follows:

$$i_{T,ads} = 2Fk_{ads}c_{H_2}[C_M(1-\theta)]^2 = 2F(k_{ads}c_{H_2}C_M^2)(1-\theta)^2 \quad (6)$$

$$i_{T,des} = 2Fk_{des}(C_M\theta)^2 = 2F(k_{des}C_M^2)\theta^2 \quad (7)$$

As suggested in Section 2.3, the concentration of dissolved gas at the reaction interface, c_{H_2}, could be considered as an unknown and cannot, therefore be evaluated independently from k_{ads} in Eq. (6). It can, however, be replaced by the product $\{c_{H_2}(c_{H_2,b})^{-1}\}c_{H_2,b}$ with, as previously suggested, $c_{H_2,b}$ ideally equal to $c_{H_2,sat}$. The empirical ratio $\{c_{H_2}(c_{H_2,b})^{-1}\}$ could be a function of current density and, for simplicity, will be represented by the symbol γ_{H_2}. The zero-current value of the ratio, $\gamma_{H_2,o}$, representing the ratio $c_{H_2,o}(c_{H_2,b})^{-1}$, should be unity. If mass transfer of dissolved H_2 to the interface is sufficiently rapid, γ_{H_2} at all current densities should be unity.

2.5.3. The Volmer equations for electron transfer

Eq. (4), with '$n = 1$' but with a stoichiometric number of 2, and with the refinements described above, leads to the following expressions for the current densities of the electron transfer (i.e. Volmer) reactions:

$$i_{V,fwd} = 2Fk_{et,fwd}(C_M\theta)\exp[\alpha_{V,fwd}F\eta(RT)^{-1}] \quad (8)$$

$$i_{V,rev} = 2Fk_{et,rev}c_{H_3O^+}\{C_M(1-\theta)\}\exp[-\alpha_{V,rev}F\eta(RT)^{-1}] \quad (9)$$

The anode activation polarization is given by η although the sign in the exponential terms of Eqs. (8) and (9) can be changed depending on the desired sign of the calculated η.

As for c_{H_2} the Tafel reaction, the concentration of hydrated protons at the reaction interface, $c_{H_3O^+}$, is unknown and cannot, therefore, be evaluated independently from $k_{et,rev}$ in Eq. (9). A combined unknown, $\{k_{et,rev}c_{H_3O^+,o}\}$ is therefore defined and an empirical ratio, $c_{H_3O^+}(c_{H_3O^+,o})^{-1}$, is proposed such that the group '$k_{et,rev}c_{H_3O^+}$' can be replaced by the group $\{k_{et,rev}c_{H_3O^+,o}\}\{c_{H_3O^+}(c_{H_3O^+,o})^{-1}\}$. For simplicity, the dimensionless ratio $c_{H_3O^+}(c_{H_3O^+,o})^{-1}$ will be represented by the symbol $\gamma_{H_3O^+}$. At zero current, $c_{H_3O^+}$ equals $c_{H_3O^+,o}$ so that $\gamma_{H_3O^+,o}$ then becomes equal to unity.

2.5.4. The Volmer reaction if Mechanism I applies

If the Volmer reactions are very fast compared to the Tafel reactions, the Tafel reactions become the rate-determining step, the forward and reverse Volmer currents are each very large compared to the Tafel currents and the Volmer reactions are at near equilibrium. In other words, equating Eqs. (8) and (9),

$$2Fk_{et,fwd}C_M \exp[\alpha_{V,fwd}F\eta(RT)^{-1}]\theta \approx 2F\{k_{et,rev}c_{H_3O^+,o}\}C_M\gamma_{H_3O} + \exp[-\alpha_{V,rev}F\eta(RT)^{-1}](1-\theta) \quad (10)$$

With the assumptions [3] that $\alpha_{V,fwd}$ equals β_V and $\alpha_{V,rev}$ equals $(1-\beta_V)$, Eq. (10) leads to the following two expressions:

$$\theta \approx \{k_{et,rev}c_{H_3O^+,o}\}(k_{et,fwd})^{-1}\gamma_{H_3O^+}\exp(-F\eta(RT)^{-1})\} \times [1+\{k_{et,rev}c_{H_3O^+,o}\}(k_{et})^{-1}\gamma_{H_3O^+}+\exp\{-F\eta(RT)^{-1}\}]^{-1} \quad (11)$$

$$\gamma_{H_3O^+} \approx \theta(1-\theta)^{-1}k_{et,fwd}\{k_{et,rev}c_{H_3O^+,o}\}^{-1}\exp\{F\eta(RT)^{-1}\} \quad (12)$$

Letting $k_{et,rev}(k_{et,fwd})^{-1}$ be represented by K_{et}, the equilibrium constant for the electron transfer reaction, Eq. (12) becomes

$$\gamma_{H_3O^+} \approx \theta(1-\theta)^{-1}\exp\{F\eta(RT)^{-1}\}\{K_{et}c_{H_3O^+,o}\}^{-1} \quad (13)$$

2.5.5. The Tafel reaction if Mechanism I applies

If the Volmer reaction is very fast relative to the Tafel reaction, the forward and reverse Volmer currents will essentially determine the value of θ. The 'slow' Tafel reaction will then be the rate-determining-step and, even though the electrons are all produced by the Volmer reaction (as seen in Section 2.2), it will be the basis for predicting the net (i.e. observed) current density. Therefore, from Eqs. (6) and (7):

$$i = 2F(k_{ads}c_{H_2}C_M^2)(1-\theta)^2 - 2F(k_{des}C_M^2)\theta^2 \quad (14)$$

2.5.6. The 'zero current, zero polarization' expressions

The exchange current density, essentially the rate of reaction in chemical kinetics terminology, reflects the kinetics of the Tafel reaction at the θ_0 condition. Here there is no net current, the exchange current density i_o is equal to both $i_{ads,o}$ and $i_{des,o,}$ and the equilibrium value of θ, θ_0, is consistent with the adsorption/desorption equilibrium given by the equality of Eqs. (6) and (7):

$$i_0 = i_{ads,0} = 2F(k_{ads}c_{H_2,b}C_M^2)\gamma_{H_2,o}(1-\theta_0)^2 \quad (15)$$

$$i_0 = i_{des,0} = 2F(k_{des}C_M^2)\theta_0^2 \quad (16)$$

By definition, $\gamma_{H_2,o}$, representing $c_{H_2,o}(c_{H_2,b})^{-1}$, is unity at zero current so that this parameter should disappear from Eq. (15). With $k_{ads}(k_{des})^{-1}$ being replaced by the adsorption equilibrium constant K_{ads}, the following equilibrium expressions result:

$$\theta_0(1-\theta_0)^{-1} = (K_{ads}c_{H_2,b})^{1/2} \quad (17)$$

$$\theta_0 = (K_{ads}c_{H_2,b})^{1/2}\{1+(K_{ads}c_{H_2,b})^{1/2}\}^{-1} \quad (18)$$

Also, from Eqs. (8), (9) and (11), θ_0 can be given by:

$$\theta_0 \approx \{K_{et}c_{H_3O^+,o}\}[1+\{K_{et}c_{H_3O^+,o}\}]^{-1} \quad (19)$$

This represents the maximum value of θ since, once current starts to flow, the discharge reaction reduces the coverage of H atoms on the surface and θ decreases from θ_0.

As the polarization approaches zero, θ in the electron transfer expressions, Eq. (13), with $\gamma_{H_3O^+}$ now also approaching unity, must approach the equilibrium, 'zero-current', value, θ_0, given by Eq. (17). This leads to the requirement that

$$\theta_0(1-\theta_0)^{-1} \approx K_{et}c_{H_3O^+,o} \quad (20)$$

Eqs. (17) and (20), therefore, imply that

$$\{K_{et}c_{H_3O^+,o}\} \approx K_{ads}^{1/2}c_{H_2,b}^{1/2} \quad (21)$$

The equilibrium constants K_{ads} and K_{et} should be functions of temperature only so that, as indicated by Eq. (21), the zero-polarization value of $c_{H_3O^+}$, $c_{H_3O^+,o}$, should adjust until it is approximately equal to the ratio $K_{ads}^{1/2}c_{H_2,b}^{1/2}(K_{et})^{-1}$ at the reaction interface. The degree of approximation depends on the relative values of the Volmer and Tafel reactions. If, for example, the forward and reverse Volmer reactions are, respectively, infinitely faster than the forward and reverse Tafel reactions, the Tafel reactions have an insignificant influence on the value of θ and the equalities in Eqs. (19)–(21) become exact.

2.5.7. Conversion to the form of a Butler–Volmer equation

Dividing Eq. (14) by Eqs. (15) and (16) leads to

$$i(i_0)^{-1} = \gamma_{H_2}(\gamma_{H_2,o})^{-1}[(1-\theta)(1-\theta_0)^{-1}]^2 - [\theta(\theta_0)^{-1}]^2 \quad (22)$$

where $\gamma_{H_2}(\gamma_{H_2,o})^{-1}$ is actually simply $c_{H_2}(c_{H_2,o})^{-1}$.

Combining Eq. (11) with Eq. (22) leads to the following expression linking current density, i, and activation polarization, η:

$$i = i_{o,T}[c_{H_2}(c_{H_2,o})^{-1}(1-\theta)^2(1-\theta_0)^{-2}]\{1-\{\gamma_{H_3O^+}\}^2 \times [\exp\{-F\eta(RT)^{-1}\}]^2\} \quad (23)$$

This is of the general form of a Butler–Volmer equation. If Eq. (23) is rearranged into the form of a Tafel equation, the following results:

$$\eta = -RT(2F)^{-1}\ln[\{\gamma_{H_3O^+}\}^{-2} \times [1-\{i(i_{o,T})^{-1}[c_{H_2}(c_{H_2,o})^{-1}(1-\theta)^2(1-\theta_0)^{-2}]^{-1}\}] \quad (24)$$

Austen [11], via a more detailed route, derived the same equations (in Section 5.9.3, Case 2A, around Eqs. (5.68)–(5.71)) and Breiter [17] presented a similar equation. For brevity, the function can be represented by the symbol f_I and the expression can be put in the traditional, 'log base 10', form so that Eq. (24) can be written

$$\eta = -2.303RT(2F)^{-1}\log[\{\gamma_{H_3O^+}\}^{-2}\{1-i(i_{o,T}f_I)^{-1}\}] \quad (25)$$

Eq. (25) provides the basis for the Tafel plot although, if $\lambda_{H_3O^+}$ and f_I are significantly different from unity, the usual 'η vs. log i' plot will not give a very accurate value of $i_{o,T}$.

3. Evaluation of Tafel–Volmer parameters from published polarization data

3.1. Introduction

The comparatively few published results on the HOR for Pt(1 1 0) were reviewed. The various thermodynamic and kinetic equations that have been derived above for the Tafel–Volmer reaction

Table 1
Exchange current densities, i_o, in A cm^{-2} for the HOR on Pt(1 1 0) from the RDE polarization data of the Markovic Group.

Temperature (K)	$i_{o,Note\ 1} \times 10^3$	$i_{o,Note\ 2} \times 10^3$	$i_{o,Note\ 3} \times 10^3$
274	0.65	1.0	0.93
303	0.98	1.35	1.45
333	1.35	1.50	1.55

Note 1: As originally recommended by the Markovic Group [4–9].
Note 2: As subsequently proposed by Mann et al. [3] based on the proposed $\eta(i)$ database in Ref. [3].
Note 3: Now proposed using the Ref. [3] 'limit method' but using the expanded $\eta(i)$ database currently proposed in Table 2.

sequence were applied and, where possible, values of the various Tafel–Volmer parameters were determined. The goal was the evaluation of parameter values for use in mechanistic equations for the prediction of η (i.e. $\eta_{act,a}$) as a function of current density (or anode activation polarization) and cell operating parameters for the HOR on Pt(1 1 0).

3.2. The original published results of the Markovic Group

The 'Markovic Group' body of work [4–9] included results at 274 K, 303 K and 333 K with the most comprehensive results being at the lowest temperature studied, 274 K. They reported the i_o results for their Pt(1 1 0) single-crystal RDE measurements that are listed in Table 1. For the reasons recently presented [3], their results were reassessed and are further discussed in Section 3.3.

The catalyst is considered as a 'reactant' and appears in kinetic expressions as a 'concentration', symbol C_M. The 'Markovic Group' concluded that, in single-crystal studies [8], well-ordered Pt($h\,k\,l$) surfaces could be produced, each Pt configuration having a particular Pt atom surface density. Of present interest is the surface density of Pt(1 1 0), which they reported as 0.94×10^{15} atoms cm^{-2}. This gave a $C_{M,1\,1\,0}$ value of 1.56×10^{-9} mol cm^{-2}, the value used in our subsequent data analyses.

3.3. Our reassessment of the published data from the 'Markovic Group'

3.3.1. Our preliminary reassessment of the 'Markovic Group' data

Our original reanalysis [3] of the published results of the Markovic Group began with the estimation of mass-transfer-corrected $\eta_{act}(i)$ data sets, shown in Table 2 for their Pt(1 1 0) electrodes, from their previously published $E(i)$ data sets. These 'extracted' $\eta_{act}(i)$ data sets were then recorrelated using Tafel–Volmer equations summarized in Section 2.

For Pt(1 1 0), assuming the 'Mechanism I' special case of the Tafel–Volmer equations at all temperatures, the i_o results listed in Table 1 were recommended from this reanalysis. These i_o results came from the following application of Eq. (23):

$$i_{o,T} = \lim_{i \to 0} [i\{1 - \exp(-2F\eta(RT)^{-1}\}^{-1}] \quad (26)$$

Accompanying this reanalysis, empirical expressions were proposed to represent the variation with current density of the group $[c_{H_2}(c_{H_2,o})^{-1}(1-\theta)^2(1-\theta_0)^{-2}]$, i.e. f_1, in Eqs. (23)–(25).

Before the kinetic and thermodynamic parameters could be quantified, a basis for the prediction of c_{H_2} had to be established.

3.3.2. Hydrogen solubility in the H_2SO_4 electrolyte and the prediction of c_{H_2}

Values of c_{H_2} are required to apply Eq. (6) and the various expressions derived from Eq. (6). For the 0.05 M H_2SO_4 electrolyte used by the Markovic Group and based on their statement that 'data were reported as adjusted to a hydrogen gas pressure of 1 atm', i.e. '$p_{H_2} = 1$', the following correlations [1] are considered to be applicable for the prediction of $c_{H_2,sat}$:

$$c_{H_2,0-45\,^\circ C} = 1.25 \times 10^{-7} \exp(545T^{-1}) \quad (27)$$

$$c_{H_2,45-100\,^\circ C} = 1.19 \times 10^{-6} \exp(-170T^{-1}) \quad (28)$$

As discussed in Section 2.3, this $c_{H_2,sat}$ should be the same as $c_{H_2,b}$ at the electrolyte/reaction boundary layer interface if diffusion in the bulk electrolyte has been properly accounted for. Further, if there is no depletion of dissolved hydrogen in the reaction boundary layer adjacent to the reaction interface, the reaction interface value, c_{H_2}, should also equal $c_{H_2,sat}$.

Eqs. (27) and (28) intersect at 45 °C so that a slight inflection point might be expected at this temperature in Arrhenius plots of parameters which vary with c_{H_2}.

3.3.3. Our present correlation of Pt(1 1 0) results by Mechanism I

Subsequent to our preliminary analysis [3], several additional $\eta(i)$ datasets were estimated from the Markovic Group $E(i)$ datasets (Table 2).

The various T–V models described in Section 2 have a large number of adjustable parameters and constraints to consider during correlation:

- the Tafel rate parameters k_{ads} and k_{des} (or, in some cases, the equilibrium parameter K_{ads});
- the Volmer rate parameters $k_{et,fwd}$ and $k_{et,rev}$ (or, in some cases, the equilibrium parameter K_{et});
- the $\gamma_{H_3O^+}(i)$ or $\gamma_{H_3O^+}(\eta)$ variation;
- the values of the transfer coefficients $\alpha_{V,fwd}$ and $\alpha_{V,rev}$;
- the desirability that the above rate parameters and equilibrium parameters show Arrhenius behaviour;
- the desirability that the parameter values resulting from the correlations predict i_o values that agree with the 'Note 3' values in Table 1.

Various combinations of Eqs. (6), (7) and (11)–(16) were applied to correlate the datasets in Table 2. Since Table 2 data were the result of a mass-transfer correction to the original $E(i)$ data, a value of unity was assumed for the parameter γ_{H_2}. The parameter $\gamma_{H_3O^+}$, however, was not necessarily subject to the assumption of unity. Values of the transfer coefficients, $\alpha_{V,fwd}$ and $\alpha_{V,rev}$, were taken to be the 0.5 value previously found satisfactory [3].

The most successful correlation technique utilized a 'general' Tafel–Volmer spreadsheet program so that k_{ads}, k_{des}, $k_{et,fwd}$, $k_{et,rev}$ and $\gamma_{H_3O^+}$ were all adjustable parameters. To convert this to a Mechanism I, 'rate determined by Tafel reaction and θ essentially determined by the Volmer reaction', values of $k_{et,fwd}$ and $k_{et,rev}$ were

Table 2
$\eta_{act,a}(i)$ data sets for Pt(1 1 0) estimated from the $E(i)$ polarization data of the Markovic Group (expanded from Ref. [3]).

274 K		303 K		333 K	
$i \times 10^3$ A cm^{-2}	$\eta \times 10^3$ V	$i \times 10^3$ A cm^{-2}	$\eta \times 10^3$ V	$i \times 10^3$ A cm^{-2}	$\eta \times 10^3$ V
0.0655	0.78	0.10	0.90	0.10	0.868
0.131	1.45	0.20	1.80	0.19	1.571
0.263	3.00	0.30	2.69	0.20	1.65
0.491	5.50	0.362	3.24	0.30	2.304
0.719	7.80	0.40	3.52	0.40	2.828
1.0	10.7	0.50	4.34	0.414	2.891
1.1	12.0	0.60	5.15	0.50	3.362
1.2	13.5	0.70	5.93	0.60	3.863
1.3	15.2	0.80	6.66	0.647	4.053
1.4	17.0	0.90	7.34	0.70	4.26
		1.00	7.95	0.80	4.65
				0.90	4.94

Several datasets have been added or slightly altered in value since Ref. [3].

Table 3
Correlation of Pt(1 1 0) $\eta(i)$ data from Table 2 using 'Mechanism I' Tafel–Volmer equations with γ_{H_2} set equal to 1 and with i_o consistent with $i_{o,Note\ 3}$ in Table 1.

T (K)	$\{K_{et}c_{H_3O^+,o}\}$ (1)	$k_{ads} \times 10^{-16}$	$k_{des} \times 10^{-9}$	$\gamma_{H_3O^+}$	$i_o \times 10^3$	$K_{ads}^{1/2}c_{H_2}^{1/2}$ (1)	θ_0
274	1.3545	1.20	5.98	1 to <1	0.93	1.3459	0.5753
303	4.800	13.8	4.51	1 to >1	1.45	4.800	0.8276
333	14.8533	119.5	3.87	1 to <1	1.60	14.809	0.9369

(1) As discussed in the paper, $K_{ads}^{1/2}c_{H_2}^{1/2}$ should be equal to $\{K_{et}c_{H_3O^+,o}\}$.

increased until variations in k_{ads} and k_{des} no longer affected the values of θ. Values of k_{ads}, k_{des}, the group $\{k_{et,rev}c_{H_3O^+,o}(k_{et,fwd})^{-1}\}$ and, when appropriate, $\gamma_{H_3O^+}$ were then varied until the best agreement of i_{pred} and i_{exp} was obtained for the datasets for a particular temperature. Typically this meant an average $i_{pred}(i_{exp})^{-1}$ of unity, an i_o value consistent with the $i_{o,Note\ 3}$ values in Table 1, and the best 'i_{pred} vs. i_{exp}' parity plot.

The data were correlated with five major constraints in mind:

(1) The resulting set of parameter values should predict values of i_o that are in close or reasonable agreement with the $i_{o,Note\ 3}$ values in Table 1.
(2) The resulting sets of k_{ads}, k_{des} and $\{k_{-et}c_{H_3O^+,o}(k_{et})^{-1}\}$ parameter values should show good Arrhenius behaviour.
(3) The values of $\gamma_{H_3O^+}(i)$ at the 3 experimental temperatures can be assumed to have an ideal value of unity.
(4) The final values of $(K_{ads}c_{H_2,b})^{1/2}$ and $\{K_{et}c_{H_3O^+,o}\}$ should be in close agreement.
(5) In addition, if $\gamma_{H_3O^+}(i)$ is a physico-chemical parameter and is not equal to unity, the final values should show a variation with temperature that was reasonable.

Several correlation approaches were applied:

(i) one that placed most emphasis on constraints (1) and (5) above;
(ii) one that placed most emphasis on constraints (2), (3) and (5) above, and
(iii) one that placed additional emphasis on constraint (5) above.

It was found that all the above constraints could not be completely met. The best correlation results are summarized in Table 3 and plotted in Fig. 1. Table 1 $i_{o,Note\ 3}$ values were met at 274 K and 303 K while an i_o value 3% higher than the $i_{o,Note\ 3}$ value gave the best results at 333 K.

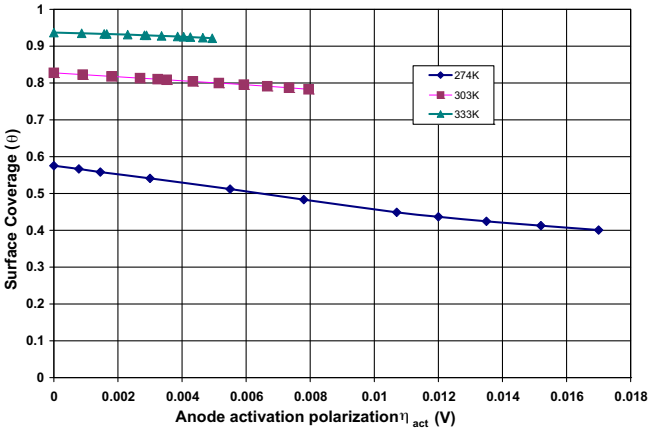

Fig. 1. Calculated values of θ_0 and θ using proposed 'Mechanism I' equations and the Tafel–Volmer parameter values in Table 3.

3.3.4. Correlation of Tafel parameters k_{ads} and k_{des}

The proposed preliminary Arrhenius correlations for the adsorption and desorption rate constants in Table 3 are, respectively:

$$k_{ads} \approx 2.37 \times 10^{27} \exp\{-7135(T)^{-1}\} \quad (29)$$

$$k_{des} \approx 5.24 \times 10^{8} \exp\{660(T)^{-1}\} \quad (30)$$

These correlations predict the experimental values of k_{ads} and k_{des} in Table 3 to within about ±2½%. This is quite reasonable for many kinetic applications but not really good enough when the current density at the anode is low and when the forward and reverse current densities can be relatively close in value. For this reason, since the probable uncertainty in the parameter values at the 3 experimental temperatures is similar, separate correlations are proposed below for the 2 temperature regions, 'below 303 K' and 'above 303 K':

$$k_{ads,<303} = 1.55 \times 10^{27} \exp\{-7013(T)^{-1}\} \quad (31)$$

$$k_{des,<303} = 3.12 \times 10^{8} \exp\{809(T)^{-1}\} \quad (32)$$

$$k_{ads,>303} = 3.83 \times 10^{27} \exp\{-7287(T)^{-1}\} \quad (33)$$

$$k_{des,>303} = 9.06 \times 10^{8} \exp\{486(T)^{-1}\} \quad (34)$$

3.3.5. Correlation of Tafel parameters K_{ads} and $\{K_{ads}c_{H_2}\}^{1/2}$

With K_{ads} defined as the ratio $k_{ads}(k_{des})^{-1}$, the following is implied by Eqs. (31)–(34):

$$K_{ads,<303} = 4.97 \times 10^{18} \exp\{-7822(T)^{-1}\} \quad (35)$$

$$K_{ads,>303} = 4.227 \times 10^{18} \exp\{-7773(T)^{-1}\} \quad (36)$$

Either by combining Eqs. (35) and (36) with Eq. (27) or (28), or by using k_{ads} and k_{des} values from Table 3, values of the equilibrium group $\{K_{ads}c_{H_2}\}^{1/2}$ can be obtained. These are listed in Table 4. Correlations for $\{K_{ads}c_{H_2}\}^{1/2}$ are not proposed since the above correlations for K_{ads} have, of necessity, been based on an inflection at 303 K while the published c_{H_2} correlations, Eqs. (27) and (28), are based on an inflection at 45 °C, i.e. 318 K.

As implied by Eq. (21), these proposed $\{K_{ads}c_{H_2}\}^{1/2}$ values should also give reasonable values of $\{K_{et}c_{H_3O^+,o}\}$. This is covered in the following section.

3.3.6. Correlation of Volmer parameter $\{K_{et}c_{H_3O^+,o}\}$

The experimental values of this parameter are listed in Table 3. They are reasonably fitted by the following Arrhenius expression:

$$\{K_{et}c_{H_3O^+,o}\} \approx 1.00(10^6) \exp\{-3704(T)^{-1}\} \quad (37)$$

Table 4
Tafel parameters K_{ads} and $(K_{ads}c_{H_2})^{1/2}$ for Pt(1 1 0).

T (K)	$k_{ads}(k_{des})^{-1} \times 10^{-7}$ (1)	$c_{H_2} \times 10^7$ (2)	$(K_{ads}c_{H_2})^{1/2}$
274	0.199	9.136	1.348
303	3.055	7.552	4.803
333	30.80	7.142	14.83

(1) From Eqs. (35) and (36).
(2) From Eqs. (27) and (28).

As for the parameter $\{K_{ads}c_{H_2}\}^{1/2}$ in the previous section, the 45 °C inflection point can be assumed giving:

$$\{K_{et}c_{H_3O^+,o}\}_{0-45\,^\circ C} = 7.46 \times 10^5 \exp\{-3620(T)^{-1}\} \quad (38)$$

$$\{K_{et}c_{H_3O^+,o}\}_{>45\,^\circ C} = 2.41 \times 10^6 \exp\{-3995(T)^{-1}\} \quad (39)$$

The two sources of $\{K_{et}c_{H_3O^+,o}\}$ values, experimental values from Table 3 and predicted $\{K_{et}c_{H_3O^+,o}\}$ values from Eqs. (38) and (39), and the predicted $\{K_{ads}c_{H_2}\}^{1/2}$ values in Table 4, are in very good agreement as expected from Eq. (21).

3.3.7. Calculation of θ_0 and θ

Values of θ_0 are estimated from Eq. (19), listed in Table 3, and plotted in Fig. 1. As expected, and consistent with Eqs. (31)–(36), the values of θ_0 increase with temperature and reach levels well above the usual 'low-coverage' referred to with Langmuir adsorption.

Values of θ were evaluated via Eq. (11) during the correlation process and representative values are also plotted in Fig. 1. These $\theta(\eta)$ plots are of relatively low slope, possibly indicating that the variation in θ is so low that non-Langmuir behaviour should not show up. This $\theta(\eta)$ variation is examined further in Section 3.3.8.

3.3.8. Correlations and parity plots at current densities above zero

In general, correlation at increasing current densities could not be attained if $\gamma_{H_3O^+}$ was constrained to a constant value of unity. As listed in Table 3, $\gamma_{H_3O^+}$ had a value at or near unity at low current density but generally required a non-unity value as current density increased if a good parity plot, i_{pred} vs. i_{exp}, was to be obtained. Graphed values of $\gamma_{H_3O^+}$ did not show a consistent variation with current density, with η or with temperature so that simple correlation was not possible or, probably, meaningful.

However, for production of a parity plot, extrapolation of the polarization curves to higher current densities or for prediction of polarization curves at other operating conditions, beginning the calculation with a value of η and then calculating the resultant current density was the simplest approach. An empirical parameter, either $\gamma_{H_3O^+}$ or θ, was therefore required as a function of η.

It became clear that $\theta(\eta)$ was the best semi-empirical function to bring in any departure of $\gamma_{H_3O^+}$ from unity, the following expressions representing the fits of the θ values required for the kinetic parameter values summarized in Table 3. It was evident that the linear $\theta(\eta)$ expression for 303 K was reasonably accurate but the linear $\theta(\eta)$ expressions for 274 K and 333 K showed deviation in opposite directions at higher values of current density. An additional small term is, therefore, proposed below for the 274 K and the 333 K empirical expressions:

$$\theta_{274\,K} \approx \theta_{0,274\,K} - 13.0\eta + 3.93 \times 10^4 \eta^{3.35} \quad (40)$$

$$\theta_{303\,K} = \theta_{0,303\,K} - 5.45\eta \quad (41)$$

$$\theta_{333\,K} \approx \theta_{0,333\,K} - 2.3\eta - 1.86 \times 10^5 \eta^{3.35} \quad (42)$$

Parity plots using the experimental results were then produced as follows:

- Eqs. (31)–(34) were applied to obtain values of k_{ads} and k_{des};
- Eqs. (27) and (28) were applied to obtain predicted values of c_{H_2};
- C_M was equal to 1.56×10^{-9};
- Eqs. (40)–(42) were applied to the experimental values of η in Table 2 to obtain predicted values of θ for each experimental data set;
- Eq. (14), with γ_{H_2} set equal to 1, was then applied to obtain predicted values of current density, i_{pred};

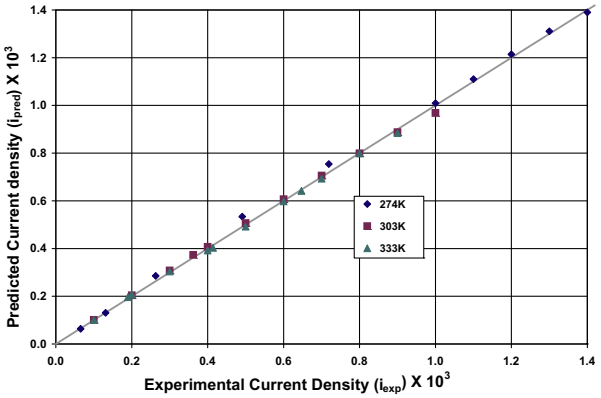

Fig. 2. Parity plot of i_{pred} vs. i_{exp} parity plot for the data in Table 2 using the proposed Mechanism I Tafel–Volmer equations and parameter values in Table 3.

The resulting values of i_{pred} were then calculated for each polarization, η_{exp}, in Table 2 and the i_{pred} vs. i_{exp} results are plotted in Fig. 2.

For greater applicability in predicting polarization curves at other operating conditions, the following generalizations are proposed to the above calculation sequence:

(a) The slopes, m_θ, in the linear term of Eqs. (40)–(42) are nearly Arrhenius in their temperature dependence and can be approximately represented by:

$$m_\theta \approx 7.39 \times 10^{-4} \exp\{2680(T)^{-1}\} \quad (43)$$

However, for greater accuracy at both interpolated and extrapolated temperatures, the following are proposed:

$$m_{\theta,<303\,K} \approx 1.475 \times 10^{-3} \exp\{2489(T)^{-1}\} \quad (44)$$

$$m_{\theta,>303\,K} \approx 3.78 \times 10^{-4} \exp\{2900(T)^{-1}\} \quad (45)$$

Similarly, the coefficients, c_θ, for the $\eta^{3.35}$ terms in Eqs. (40)–(42) can be generalized somewhat via the following:

$$c_{\theta,<303\,K} \approx -1.36(10^3)T + 4.12(10^5) \quad (46)$$

$$c_{\theta,>303\,K} \approx -6.2(10^3)T + 1.88(10^6) \quad (47)$$

Thus, $\theta(\eta)$ can be estimated via Eq. (19), Eqs. (44)–(47), and

$$\theta = \theta_0 - m_\theta \eta + c_\theta \eta^{3.35} \quad (48)$$

3.3.9. Calculation of i_{pred} for a given temperature (25 °C) and a given value of η

The calculation sequence proposed in Section 3.3.8 was applied to the prediction of all parameter values for 25 °C and an anode activation polarization, η, of 1×10^{-3} V. The applicable equation numbers and the results are summarized in Table 5.

The same process summarized in Table 5 was applied to the prediction of the polarization curve for 'Pt(1 1 0), 25 °C, $p_{H_2} = 1$ atm, $C_M = 1.56 \times 10^{-9}$ using the parameter values in Table 5 and applying Eq. (14). The results are summarized in Fig. 3.

3.4. Analysis of the published Pt(1 1 0) data from Protopopoff and Marcus (1985–1988)

Protopopoff and Marcus, in a series of papers, studied the influence of sulphur on the electroadsorption of hydrogen under the H^+:H_2 equilibrium potential [20,21] and on the HER [22] on a single-crystal Pt(1 1 0) surface. Results at zero sulphur were also reported so that there are some data that are relevant to the present paper. Experimental conditions for the HER study were 25 °C, 0.05 M H_2SO_4 aqueous electrolyte, and, presumably, a p_{H_2}

Table 5
Estimation of parameter values at 25 °C and $\eta = 1 \times 10^{-3}$ for Pt(1 1 0) with dilute H_2SO_4 electrolyte and $C_M = 1.56 \times 10^{-9}$.

Parameter	Source	Estimated value	Note
m_θ	Eq. (44)	6.254	
c_θ	Eq. (46)	6.72×10^3	
$\{K_{et} c_{H_3O^+,o}\}$	Eq. (38)	3.9544	(1)
θ_0	Eq. (19)	0.79816	
θ	Eq. (48)	0.7919	
k_{ads}	Eq. (31)	9.329×10^{16}	
k_{des}	Eq. (32)	4.7115×10^9	
c_{H_2}	Eq. (27)	7.783×10^{-7}	
$[k_{ads} c_{H_2} (k_{des})^{-1}]^{1/2}$	Calc'd	3.9196	(1)
i_{pred} ($\gamma_{H_2,o} = 1$)	Eq. (14)	8.9×10^{-5}	
$i_{o,fwd}$ ($\gamma_{H_2,o} = 1$)	Eq. (15)	1.389×10^{-3}	(2)
$i_{o,rev}$	Eq. (16)	1.388×10^{-3}	(2)

(1) For internal consistency, $(k_{ads} c_{H_2}/k_{des})^{1/2}$ and $\{K_{et} c_{H_3O^+,o}\}$ should be close in value.
(2) For the parameter values to show complete internal consistency, $i_{o,fwd}$ and $i_{o,rev}$ should have identical values.

of 1 atm. Current densities were calculated on the basis of the geometric area of the electrode. The Tafel slope for the zero-S polarization curve was 0.035 ± 0.001 V dec^{-1} and the current density at 0 V was $(1.7 \pm 0.05) \times 10^{-4}$ A cm^{-2}. The 0.035 was considered by the authors to be close enough to the 0.0296 value that would come from our Eq. (29) to support this HER as a 'proton discharge in equilibrium followed by rate-determining chemical recombination' (i.e. our Mechanism I in reverse). They cited some additional supporting literature [23–26] but it does not appear that any of this work involved single-crystal Pt(1 1 0).

As recently argued [3], a 'modified Tafel plot' according to Eqs. (24) and (25) should be based on η being plotted against $\log[i(f_l)^{-1}]$, not $\log[i]$, a procedure that will modify the resulting values of both the Tafel slope (i.e. α) and the Tafel intercept (i.e. i_o).

The concept of exchange current density, the equal forward and reverse current densities at zero polarization and zero net current, implies that the equilibrium rate of the HOR, Eq. (2), is the same as the equilibrium rate of the HER, the reverse of Eq. (2). If the mechanism, as argued above, is the same for the HER and the HOR in the equilibrium region, the $i_{o,HER}$ and $i_{o,HOR}$ should have the same value at the same test conditions. Therefore $i_{o,HOR,298\,K}$ should also be 1.7×10^{-4} for the test parameters used in the work and for the geometric area of the electrode being used.

The evaluation of any Tafel–Volmer parameters for comparison with our results in Section 3.3 is hindered by the lack of any mention of a value of C_M for their Pt(1 1 0) electrode. Since their i_o value appears to be nearly an order of magnitude less than those proposed in Table 1, either C_M or some other experimental parameters were considerably different than those in the studies by the Markovic Group.

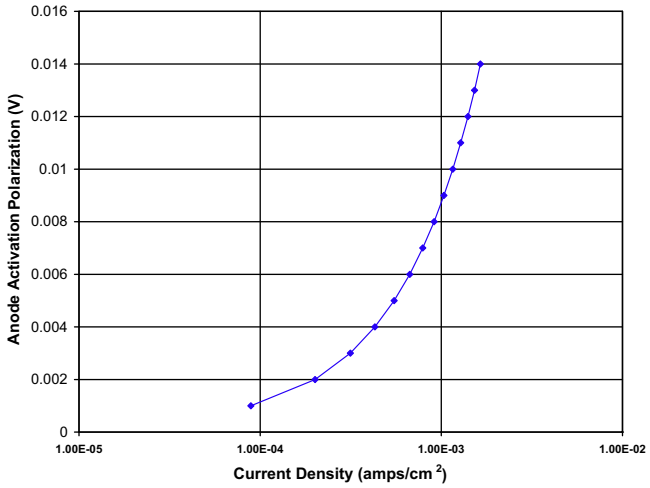

Fig. 3. Predicted polarization curve at 25 °C for the conditions in Table 5.

3.5. Analysis of the 1993 published Pt(h k l) data from Gomez et al.

Gomez et al. [27] studied the rate of the HER in 0.5 M H_2SO_4 and "arbitrarily took i_o as the current density at $E = 0$". The "room temperature" results, i_o (in A cm^{-2}) and Tafel slope, b (in V dec^{-1}), for the three basal Pt orientations were:

Pt(1 1 1): 0.84×10^{-3} and 0.030
Pt(1 0 0): 0.84×10^{-3} and 0.031
Pt(1 1 0): 0.97×10^{-3} and 0.030

The almost identical Tafel slope of ~0.03 for all three crystal orientations, especially considering the results of the Markovic Group [4–9], probably implies that the measurements were concentration polarization (i.e. mass transfer) limited. As recently noted [3], the concentration polarization expression also begins with a $2.303RT(2F)^{-1}$ term so that a diffusion-limited electrode reaction will show an apparent Tafel slope of $\sim 9.92 \times 10^{-5} T$, from 0.0289 to 0.0296 at room temperatures from 18 to 25 °C. For this reason, the results of Gomez et al. were not further evaluated.

4. Generalizations for modelling the HOR on Pt(1 1 0)

4.1. Modelling in dilute H_2SO_4 electrolytes

The implicit assumptions at this point are (i) that the HOR reaction on a Pt(1 1 0) anode is a Tafel–Volmer reaction sequence with a 'Mechanism I', rds Tafel followed by fast Volmer, process; (ii) that the dissociative chemisorption of the H_2 molecule follows a Langmuir isotherm, and (iii) the proposed parameter values and correlations in Section 3.3 apply to the 'Markovic Group' conditions for their Pt(1 1 0) anode: 0.05 M H_2SO_4, p_{H_2} of 1 atm and C_M equal to 1.56×10^{-9} mol cm^{-2}.

Generalizing $c_{H_2,o}$ to p_{H_2} other than 1 atm requires evaluation of an appropriate Henry's Law constant. As noted in Section 3.3.2 with respect to Eq. (27), Eq. (28) and to previous work [1], given the electrolyte, the temperature and the value of p_{H_2}, the value of $c_{H_2,o}$ can be estimated.

Generalizing to anode Pt(1 1 0) catalysts other than 'Markovic Group Pt(1 1 0)' requires adjustment of the value of C_M. Eqs. (15) and (16) indicate that i_o varies as C_M^2 so that a Pt(1 1 0) anode catalyst with a C_M value other than the 'Markovic Group', 'MG', value proposed in Section 3.2 would need another parameter added, $C_{M,actual}$ instead of $C_{M,MG}$, to properly scale the predicted i_o and i values. It should be noted that these C_M values are best visualized as being 'per cm^2 of geometric Pt electrode area'.

Values of $\{K_{et} c_{H_3O^+,o}\}$ for Pt(110) when p_{H_2} is other than 1 atm would also require adjustment. As noted following Eq. (12), K_{et} represents the group $\{k_{et,rev}(k_{et,fwd})^{-1}\}$ where $k_{et,rev}$ and $k_{et,fwd}$ should only be functions of temperature. As noted around Eqs. (20) and (21), $K_{et} c_{H_3O^+,o}$ should be numerically equal to $K_{ads}^{1/2} c_{H_2}^{1/2}$ and, since K_{ads} should only be a function of temperature, $c_{H_3O^+,o}$ should therefore vary as $c_{H_2}^{1/2}$, i.e. as $\{p_{H_2}(H_{H_2})^{-1}\}^{1/2}$. This means that, for a 'new' value of p_{H_2} other than the Markovic Group "adjusted to a p_{H_2} of 1 atm" 'MG' condition,

$$\{K_{et} c_{H_3O^+,o}\}_{p_{H_2}} \approx \{K_{et} c_{H_3O^+,o}\}_{p_{H_2}=1\,atm} [p_{H_2} H_{H_2,MG} (H_{H_2,new})^{-1}]^{1/2} \quad (49)$$

Eq. (49), when combined with the '$p_{H_2} = 1$ atm' results in Table 3 or with Eq. (39) for temperatures above 45 °C, leads to the following general correlation:

$$\{K_{et}c_{H_3O^+}\}_{p_{H_2},>45\,^\circ C} \approx 2.41 \times 10^6[p_{H_2}H_{H_2,MG}(H_{H_2,new})^{-1}]^{1/2} \times \exp[-3995(T)^{-1}] \quad (50)$$

The values of Henry's constant, H_{H_2}, in Eq. (50) can be evaluated for the particular electrolyte as described elsewhere [1].

4.2. Generalizing to electrolytes other than H_2SO_4

The first key parameter here is c_{H_2} and this can be evaluated for various concentrations of other acids and for Nafion membrane electrolytes by making use of the Henry's Law correlations recently proposed [1]. As long as the pH is still in the same general range as that for the dilute H_2SO_4 results, it can be assumed, until relevant experimental data are available and appropriately analysed, that the various Tafel–Volmer '$p_{H_2} = 1$' parameter values are not significantly changed from the correlations presented above. If the pH is significantly different than that in the 'Markovic Group' studies, generalization from the results in Section 3.3 should be done with caution.

The other possibility is that the reaction mechanism, and therefore the values of the kinetic parameters, differ when the ionic makeup of the electrolyte changes. In this case, the parameters derived from the H_2SO_4 studies would not likely apply.

5. Summary and conclusions

Additional support has been provided for the main assumptions: (i) that the HOR reaction on a Pt(1 1 0) anode is a Tafel–Volmer reaction sequence with a 'Mechanism I', rds Tafel followed by fast Volmer, process and (ii) that the dissociative chemisorption of the H_2 molecule follows a Langmuir isotherm [5]. These conclusions apply to the 'Markovic Group' conditions for their Pt(1 1 0) anode: 0.05 M H_2SO_4, p_{H_2} of 1 atm and C_M equal to 1.56×10^{-9} mol cm^{-2}.

Satisfactory Arrhenius correlations of several Tafel–Volmer kinetic and thermodynamic parameters for Pt(1 1 0) have been obtained for the temperature range from 1 °C to 60 °C and for the 'adjusted to a p_{H_2} of 1 atm' condition used by the 'Markovic Group' publications. This includes the parameters $\{K_{et}c_{H_3O^+}\}$, K_{ads}, k_{ads}, and k_{des}. It is suggested, pending the availability of data for Pt(1 1 0) electrodes at temperatures above 60 °C, that these correlations can be extrapolated for use at 60–90 °C, a typical operating temperature range for PEM fuel cells.

Correlations are proposed for predicting the performance of Pt(1 1 0) electrodes at p_{H_2} values of other than 1 atm and for C_M values other than that recommended by the Markovic Group.

For modelling purposes, the simplest approach for current density 'i' to be predicted as a function of anode activation polarization η. Alternatively, η can be predicted as a function of current density but this approach would require an iterative solution. A calculation sequence is proposed in Section 3.3.8.

There appears to be a surprisingly small amount of published work regarding the hydrogen oxidation reaction on Pt(1 1 0) anodes other than the several publications of the 'Markovic Group'.

It is suggested that these Tafel–Volmer parameter values can also be used to estimate $\eta(i)$ data for Pt(1 1 0) electrodes using other electrolytes in the same low-pH region as the 0.05 M H_2SO_4 cells employed by the Markovic Group. This could include PEM electrolytes such as Nafion although further work is needed to verify this approach. The major additional requirement would be the prediction of c_{H_2} values via Henry's Law expressions for the different electrolytes, a question that has recently been addressed [1].

Acknowledgement

This work has been supported by the Canadian Department of National Defence through funding supplied by Defence Research and Development Canada.

References

[1] R.F. Mann, J.C. Amphlett, B.A. Peppley, C.P. Thurgood, J. Power Sources 161 (2006) 768–774.
[2] R.F. Mann, J.C. Amphlett, B.A. Peppley, C.P. Thurgood, J. Power Sources 161 (2006) 775–781.
[3] R.F. Mann, J.C. Amphlett, B.A. Peppley, C.P. Thurgood, J. Power Sources 163 (2007) 679–687.
[4] H.A. Gasteiger, N.M. Markovic, P.N. Ross, J. Phys. Chem. 99 (1995) 8290–8301.
[5] N.M. Markovic, B.N. Grugur, P.N. Ross, J. Phys. Chem. 101 (1997) 5405.
[6] N.M. Markovic, T.J. Schmidt, B.N. Grgur, H.A. Gasteiger, R.J. Behm, P.N. Ross, J. Phys. Chem. B 103 (1999) 8568–8577.
[7] N.M. Markovic, P.N. Ross, Surf. Sci. Rep. 45 (2002) 121.
[8] N.M. Markovic, The hydrogen electrode reaction and the electrooxidation of CO and H_2/CO mixtures on well-characterized Pt and Pt-bimetallic surfaces, 2003, Chapter 26 of Volume 2 of Veilstich et al. [9].
[9] W. Vielstich, H. Gasteiger, A. Lamm (Eds.), Handbook of Fuel Cells—Fundamentals, Technology and Applications, vols. 1–4, John Wiley & Sons Ltd., 2003.
[10] R. Parsons, Trans. Faraday Soc. 54 (1958) 1053–1063.
[11] L.G. Austen, The Electrochemical Theory of Fuel Cells, in Berger [12].
[12] C. Berger (Ed.), Handbook of Fuel Cell Technology, Prentice-Hall, Englewood Cliffs, NJ, 1968.
[13] J.O'M. Bockris, A.K.N. Reddy, Modern Electrochemistry, vols. 1&2, Macdonald, Plenum Press, London, New York, 1970.
[14] E. Gileadi, E. Kirowa-Eisner, J. Penciner, Interfacial Electrochemistry: An Experimental Approach, Addison-Wesley, 1975.
[15] T.E. Springer, T. Rockward, T.A. Zawodzinski, S. Gottesfeld, J. Electrochem. Soc. 148 (1) (2001) A11–A23.
[16] G.A. Camara, E.A. Ticianelli, S. Mukerjee, S.J. Lee, J. McBreen, J. Electrochem. Soc. 149 (6) (2002) A748–A753.
[17] M.W. Breiter, Reaction mechanisms of the H_2 oxidation/evolution reaction, 2003, Chapter 25 of Volume 2 of Veilstich et al. [9].
[18] A. Lasia, Hydrogen evolution reaction, 2003, Chapter 29 of Volume 2 of Veilstich et al. [9].
[19] K.J. Vetter, in: S. Bruckensein, B. Howard, Trans. (Eds.), Electrochemical Kinetics, Academic Press, New York, 1967, pp. 516–614, in particular pp. 550–551.
[20] P. Marcus, E. Protopopoff, Surf. Sci. 161 (1985) 533–552.
[21] E. Protopopoff, P. Marcus, Surf. Sci. 169 (1986) L237–L244.
[22] E. Protopopoff, P. Marcus, J. Electrochem. Soc. 135 (1988) 3073–3075.
[23] J.O'M. Bockris, I.A. Ammar, A.K.M.S. Huq, J. Phys. Chem. 61 (1957) 879–886.
[24] S. Schuldiner, J. Electrochem. Soc. 106 (1959) 891.
[25] V.S. Bagotsky, Yu.B. Vassiliev, I.I. Pyshnograeva, Electrochim. Acta 16 (1971) 2141–2167.
[26] B.E. Conway, L. Bai, J. Electroanal. Chem. 198 (1986) 149–175.
[27] R. Gomez, A. Fernandez-Vega, J.M. Feliu, A. Aldaz, J. Phys. Chem. 97 (1993) 4769–4776.